

## GRAVITATIONAL QUANTUM STATES OF NEUTRONS AND THE NEW GRANIT SPECTROMETER

V. V. NESVIZHEVSKY (On behalf of the GRANIT Collaboration)

*Institut Laue-Langevin, 6 rue Jules Horowitz, F-38042, Grenoble, France*  
*nesvizhevsky@ill.fr*

Received 29 December 2011

Published 20 January 2012

The review covers recent developments on gravitational quantum states of neutrons and the new GRANIT spectrometer, discussed during the Workshop GRANIT-2010 in Les Houches.<sup>1</sup> The GRANIT facility<sup>2</sup> includes the spectrometer and the infrastructure needed for its operation. It is constructed at Institut Laue-Langevin (ILL)<sup>3</sup> in Grenoble for studies of/with gravitational quantum states of neutrons, and for related topics. New methodical developments<sup>4</sup> are discussed for future upgrades of this facility. An important motivation for this activity consists in constraining fundamental short-range forces.<sup>5</sup> Other quantum phenomena in gravitational field,<sup>6</sup> and centrifugal quantum states of neutrons,<sup>7</sup> were discussed as well. A detailed presentation of all these topics could be found in Workshop-2010 presentations.<sup>8</sup> We will focus here on instrumental developments and on options for studying neutron gravitational states.

*Keywords:* Gravitational quantum states; ultracold neutrons; short-range fundamental interactions; GRANIT facility.

### 1. Introduction

The Workshop GRANIT-2010 on experimental and theoretical approaches to neutron quantum states in the gravitational field took place in Les Houches, France, on 14–19 February 2010<sup>1</sup>; it was attended by over 50 participants from 12 countries. Ultracold neutrons (UCNs)<sup>9–11</sup> are settled in gravitational quantum states<sup>12–14</sup> if they are confined between a horizontal reflecting neutron mirror on bottom, and the Earth's gravitational field on top. The energy of UCNs is so low ( $\sim 10^{-7}$  eV) that they are reflected from many materials at any incidence angle due to their multiple scattering on nuclei in the material; one often discuss such scattering in terms of the optical potential of materials. If the mirror is sufficiently flat and uniform, UCNs are reflected to the specular direction. A classical analog of this phenomenon is a ping-pong ball bouncing on a surface with negligible dissipation of energy. The quantum limit is bouncing UCNs with the energy of vertical motion close to  $\sim 10^{-12}$  eV, or with the raising height close to  $\sim 10$   $\mu\text{m}$  in the Earth's gravitational field. Such

gravitational quantum states of matter were first observed in a series of experiments<sup>15–18</sup> at the Institut Laue-Langevin<sup>3</sup> (ILL). Overviews of these experiments and of physics relevant to this observation could be found, for instance, in Refs. 19 and 20. Serious efforts are devoted to confirm this observation as well as to develop the method of quantum gravitational spectroscopy for various applications; see, for instance, Refs. 21–23. In particular, the method of gravity-resonance-spectroscopy was proposed in Ref. 24 and realized recently in Ref. 25.

The aim of the GRANIT-2010 Workshop was to discuss the scientific program for the new gravitational spectrometer GRANIT.<sup>2,4</sup> The behavior of UCN in the gravitational field in GRANIT and in alternative experiments, as well as applications of this phenomenon/spectrometer to various domains of physics, ranging from constraints for short-range interactions<sup>5</sup> to neutron quantum optics and reflectometry using UCN are presented. Scientific issues, instrumental and methodical developments, alternative methods, new ideas etc. were the main topics discussed.<sup>6,7</sup> The present review mainly consists of three sections corresponding to the first three days of the Workshop; the title of each section repeats the generic title of talks given during the corresponding day. The first day was devoted to a detailed presentation of the new GRANIT spectrometer; the talks covered the engineering and methodical aspects as well as the theoretical analysis of its operation and first measurements to carry out using GRANIT. During the second day, we discussed various new methodical developments to be used for GRANIT later, in particular, real-time position-sensitive detectors of high spatial resolution, nanoparticle neutron reflectors, a new concept of a “virtual cold neutron source” for producing high UCN densities, and an option to use the GRANIT installation as a UCN reflectometer. Presentations during the third day focused on fundamental applications of GRANIT, in particular on theoretical motivations and experiments constraining short-range forces. Competing approaches using other experiments and techniques were covered, in particular the method of neutron scattering, neutron experiments based on neutron EDM setups; studies of Casimir forces and gravity at short distances, and measurements with polarized and unpolarized atoms. A broad range of alternative quantum phenomena and experiments in gravitational field were analyzed on the fourth day; attention was devoted to common problems, experimental techniques and applications of these experiments. The recently observed phenomenon of centrifugal quantum states of neutrons (neutron whispering gallery), as well as a photon bouncing ball, was presented during the fifth day of the Workshop. For the last two days, and also partly for the third day, we refer readers to proceedings and materials of the GRANIT-2010 Workshop<sup>8</sup> as their subjects deviate from the title proposed for the present review; besides, these topics are presented in the proceedings in details.

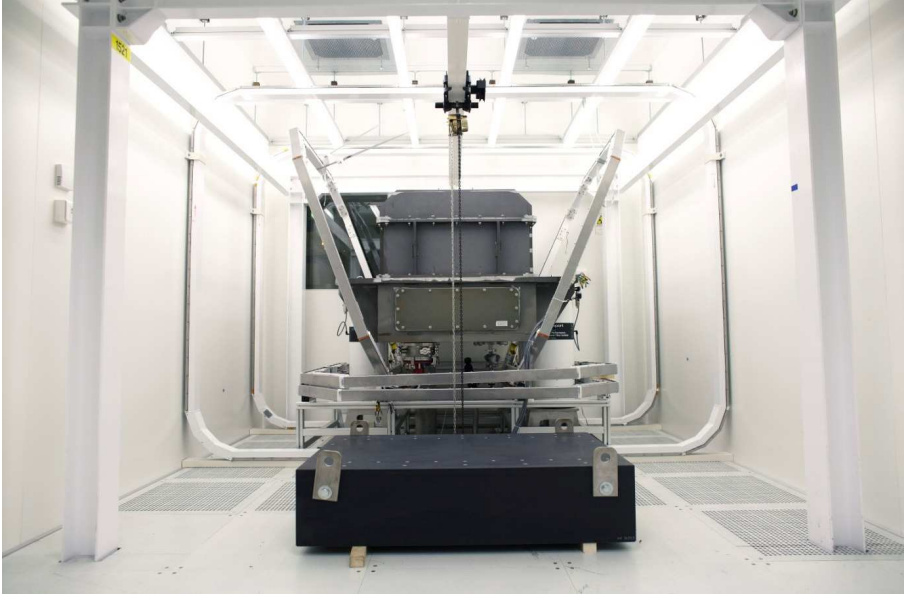


Fig. 1. The GRANIT spectrometer during its assembling, inside the GRANIT clean room.

## 2. The New GRANIT Spectrometer

After the first observation of gravitational quantum states of neutrons in the gravitational spectrometer,<sup>15</sup> the GRANIT is a follow-up project based on a second-generation spectrometer with ultra-high energy resolution<sup>2</sup> (see Fig. 1). It will provide more accurate studies of/with gravitational quantum states of UCN, in particular measurements of resonance transitions<sup>23,2</sup> between them and their interference, in analogy to the neutron whispering gallery phenomenon.<sup>26-28</sup> The GRANIT spectrometer will benefit from its permanent installation at the ILL high-flux reactor,<sup>29</sup> from a dedicated  $^4\text{He}$  UCN source<sup>30</sup> delivering UCN to the GRANIT spectrometer, with no significant dilution of the phase-space density.<sup>31,32</sup> The key property of the GRANIT spectrometer is UCN storage in gravitational bound states for extended periods using a closed specular trap. According to the uncertainty principle, longer observation time provides better defined energy and thus higher measurement precision. External perturbations, such as vibrations or gradients and time variation of the magnetic field, have to be minimized. As the fraction of gravitationally bound neutrons is extremely small, we develop neutron detectors with extremely low backgrounds, UCN sources with high phase-space density, and neutron transport systems with low losses.<sup>4</sup> The GRANIT spectrometer will be a unique tool for carrying out a wide range of investigations in fundamental physics, in foundations of quantum mechanics, in surface physics, as well as for development of experimental techniques, for physical modeling and for applications.<sup>24,19,20,33,5</sup>

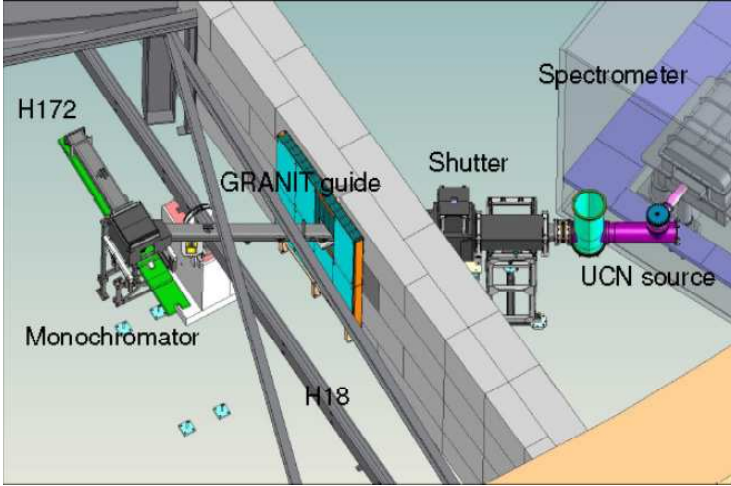


Fig. 2. A scheme of installation of the GRANIT spectrometer in the ILL reactor hall.

### 2.1. Infrastructure for the GRANIT spectrometer in ILL

Compared to preceding experiments with the gravitational spectrometer<sup>15</sup> in a temporary position at PF2 beam at ILL, the new GRANIT spectrometer gets higher statistics due to longer measuring time and a dedicated UCN source<sup>30</sup>; profits from lower vibration-noise and magnetic-noise environment, as well as from clean-room conditions needed to work safely with precision optical components. A general scheme of installation of the GRANIT spectrometer is shown in Fig. 2. Cold neutrons from the liquid-deuterium cold source in the ILL reactor are delivered, to the intercalated graphite monochromator,<sup>34</sup> which reflects neutrons with the wavelength of 8.9 Å toward <sup>4</sup>He-filled cryostat,<sup>30</sup> where they are down-scattered to UCN energies; UCNs are extracted from the cryostat and transported toward the GRANIT spectrometer, installed inside the GRANIT clean room.

### 2.2. The GRANIT spectrometer

A general view of the GRANIT spectrometer, in its simplest configuration, is given in Fig. 3; the optical components are shown in more detail in Fig. 4. The spectrometer consists of several neutron-optics elements and UCN detectors installed on a massive granite table in an aluminum vacuum chamber: (i) A mechanically-flexible neutron guide between the UCN source and the intermediate UCN storage volume; (ii) A neutron extraction system based on the method of semi-diffusive slits<sup>31,32</sup>; (iii) A transport mirror system, which can be used also for experiments with gravitational quantum states of neutrons in the flow-through mode; (iv) The main specular trap (see Fig. 4 and the inset in Fig. 3) for extended storage of UCNs in gravitational quantum states; (v) A resonant transition system,<sup>23</sup> based in first experiments on spatially varying gradients of magnetic field; (vi) Detectors of different

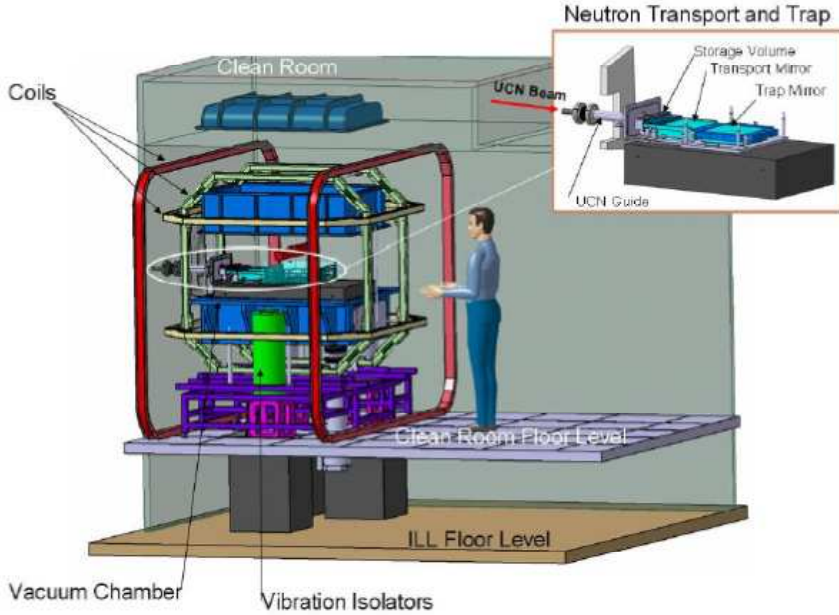


Fig. 3. A general view of the GRANIT spectrometer; the granite table supporting all mirrors and other equipments is shown in the inset.

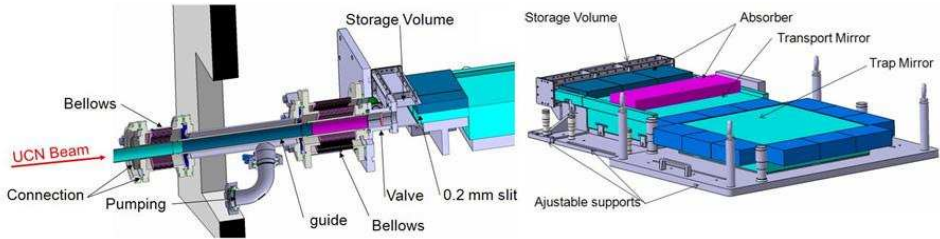


Fig. 4. From the source (left) to the trap (right): UCN guide, UCN valve, intermediate UCN storage, UCN extraction system, UCN storage trap.

type:  $^3\text{He}$  low-background proportional counters,<sup>4</sup> position-sensitive nuclear-track detectors,<sup>15</sup> real-time position-sensitive detectors; (vii) Numerous spectrum-shaping and spectrum-analyzing devices, leveling and positioning systems. The GRANIT spectrometer is equipped with (i) anti-vibration and leveling systems; (ii) clean-room; (iii) magnetic field control system.

### 2.3. Mirrors for the GRANIT Spectrometer

The key element of the GRANIT spectrometer is a set of mirrors to shape/analyze neutron spectra and to store neutrons in quantum states. The transport system

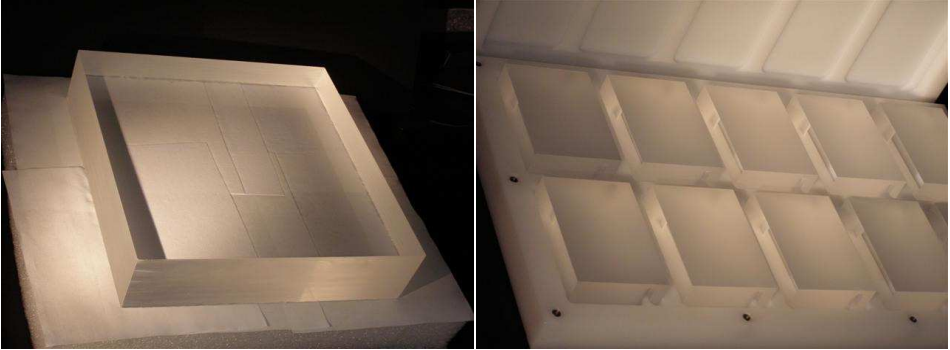


Fig. 5. Mirrors for the main trap, before coating and gluing.

consists of a bottom mirror of 30 cm by 25 cm and two side mirrors along the side of 25 cm. For the main storage mirror, a trap consists of a bottom mirror 30 cm by 30 cm, and 12 side mirrors glued together (3 mirrors per a side wall). Mirror quality, in particular the geometric shape, surface polishing, purity of the mirrors, and properties of the coatings are of major importance for the efficiency (resolution, precision, count rate) of the GRANIT spectrometer. Dedicated theoretical<sup>35</sup> and experimental<sup>36,37</sup> studies were devoted to optimize and characterize these parameters. After performing these studies we ordered the mirrors for GRANIT with suitable specifications from SESO. Produced mirrors for the main trap, before coating and gluing, are shown in Fig. 5. Diamond-like coating (DLC) of the mirrors, needed to increase critical velocity of the trap walls, is in progress in LMA.

#### 2.4. *Magnetically-induced transitions between quantum states*

A convenient method to induce resonant transitions between quantum states, at least at the first stage of our experimental program, is provided by a magnetic field gradient, which varies in space or in time. A scheme intended for first observing resonant transitions between different gravitational quantum states of neutrons in the GRANIT spectrometer is described in detail in Refs. 23 and 2 and sketched in Fig. 6. UCNs with appropriate horizontal velocity will be affected by the gradient of magnetic field that oscillates — in the reference frame of the incoming neutron — with frequency corresponding to a transition between two gravitational quantum states. In the position-sensitive detector installed after the “free fall” region, an UCN will be detected at a height, which depends on its horizontal velocity. Thus we could measure the frequency of a resonant transition.

#### 2.5. *Feasibility of mechanically-induced transitions*

An alternative method to induce transitions between quantum states could consist of mechanical oscillations of the mirror with a resonance frequency.<sup>24,25</sup> In order to

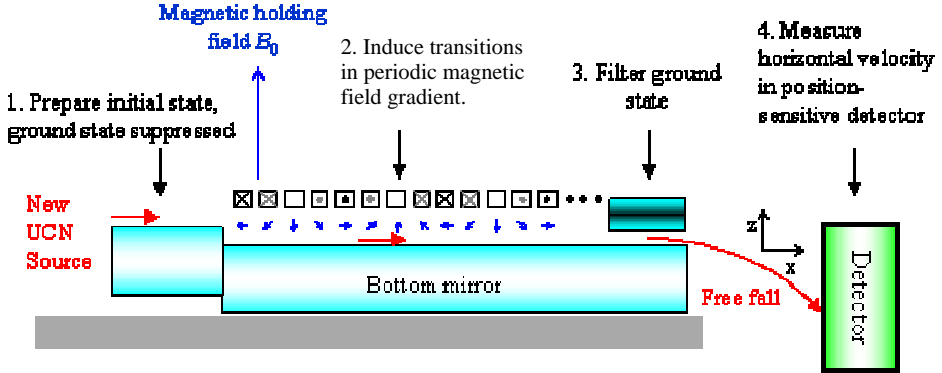


Fig. 6. A setup to detect resonance transitions in a flow-through mode with the GRANIT spectrometer. The setup is optimized in region 1 to provide neutrons mostly in the 3rd quantum state. The magnetic field in the transition region 2 rotates 20 times, each rotation takes  $\lambda = 1$  cm. The rotating magnetic field is provided by wires with a current  $I_0; 0.7I_0; 0; -0.7I_0; -I_0; -0.7I_0; 0; \dots$ . The filter in region 3 is optimized to transmit only the ground state.

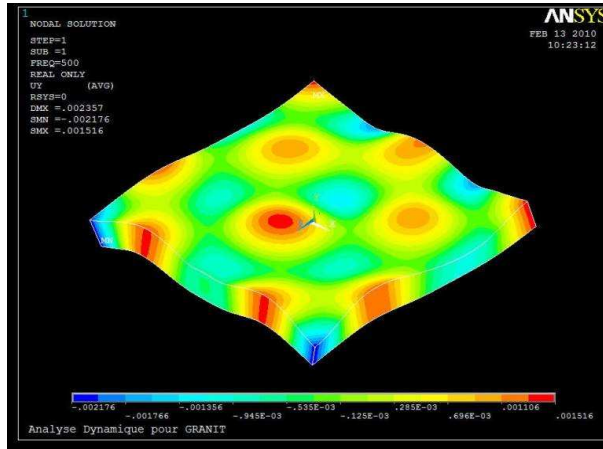


Fig. 7. (color online) Surface profile of the silica substrate, excited with three piezo-electric actuators (one at the front side and two at the back side) with a frequency of 500 Hz. The color signifies deformations with a  $3 \mu\text{m}$  peak-to-peak variation.

access the feasibility of this method in the flow-through measuring mode, as well as to estimate eventual false effects, we simulated the response of a mirror to mechanical vibrations for typical parameters of the problem, see Fig. 7. The characteristic amplitude of vibrations is estimated from the condition of the transition probability close to unity for the time of UCN passage above the mirror. The pattern of deformation depends on the excitation frequency and on parameters of the mirror and its fixation. However, the deformation is unacceptably high for precision experiments, although observation of transitions in the flow-through mode is feasible.<sup>25</sup> Thus we rejected this option for the flow-through experiments.

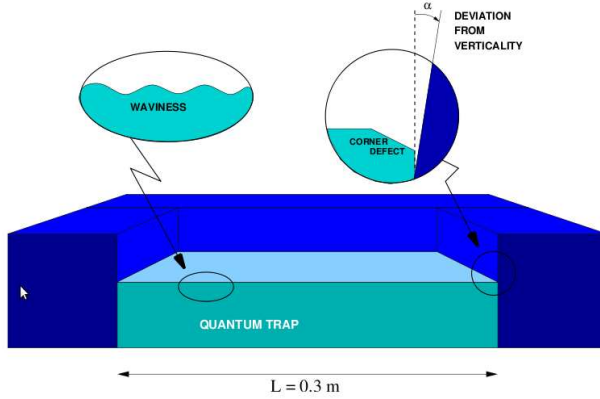


Fig. 8. Scheme of the GRANIT trap with a horizontal mirror and side walls.

*Sapphire mirrors* have been extensively used in UCN experiments including GRANIT: for efficient specular reflection<sup>37,36</sup>; and for storage of UCN in a trap.<sup>38,39</sup> This is due to the fact that sapphire provides a set of properties important for UCN experiments: in contrast to coatings and optical glasses, it survives in high radiation fluxes and at low temperatures; its mechanical hardness, in contrast to metals and coatings, allows one to polish its surface to a few angstrom roughness and keep it intact in numerous mechanical manipulations; its effective optical potential of  $1.5 \cdot 10^{-7} \text{ eV}$  is quite high compared to those for glasses and silicon; its surface, in contrast to metals and coatings, is free from major contaminations and nanostructures.

## 2.6. Analysis of storage times of UCN in gravitational quantum states

When measuring the energy levels of neutron gravitational quantum states using the resonant transition method, one main parameter is the time available to excite a given transition: precision experiments are conditioned by long storage of UCN in a quantum state and weak perturbation leading to the resonant transition. Consider the main trap with geometry shown in Fig. 8. The lifetime of the neutron quantum states in such a trap has been estimated for different relevant sources of loss.<sup>40,35</sup> The results, for typical experimental conditions achievable with the GRANIT spectrometer, are summarized in Fig. 9. As you can see, the possible storage times are quite long, particularly for lowest quantum states, compared to  $\sim 50 \text{ ms}$  achieved in Refs. 16–18.

## 2.7. Theory of interaction of UCN in gravitational quantum states with absorber

An important ingredient of experiments with neutron gravitational states is selection of one or a few quantum states. In the experiments performed earlier<sup>16–18,22</sup>



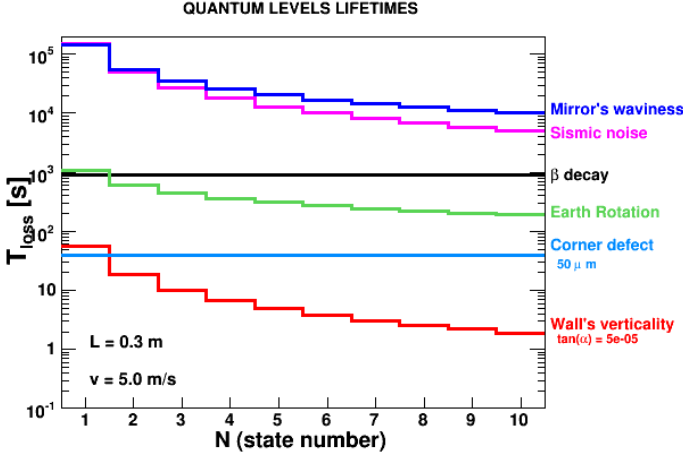


Fig. 9. Estimated lifetime of 10 lowest quantum states due to various systematic effects.

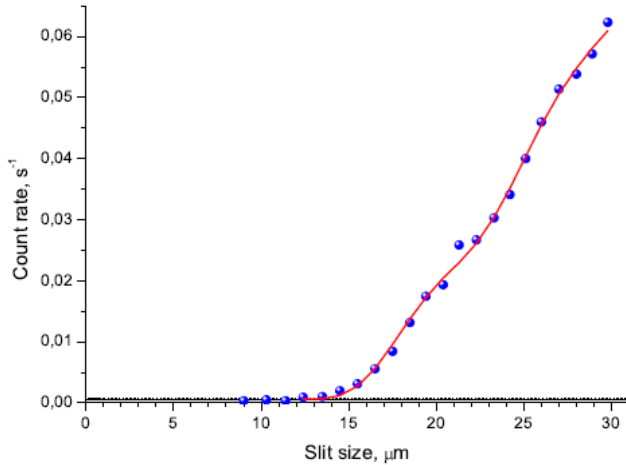


Fig. 10. Neutron count rate at the exit of the waveguide, formed by a mirror on bottom and a scatterer/absorber on top, as a function of the absorber position. Circles correspond to the experimental data; solid line shows the theoretical model. The figure is copied from Ref. 18.

selective action of rough absorber on different gravitational quantum states was achieved by adjusting the absorber height above mirror to the neutron gravitational state spatial size. Neutrons in states with the spatial size smaller than the absorber height are weakly affected, while those with larger size are intensively absorbed. The quantitative theory of this quite complex process is important for precision analysis of the data. It has been developed in detail in Refs. 41–44. An example showing agreement between experimental data and theoretical models is given in Fig. 10; here we see the transmission of UCNs through a waveguide between a polished mirror on bottom and a rough absorber/scatterer on top.

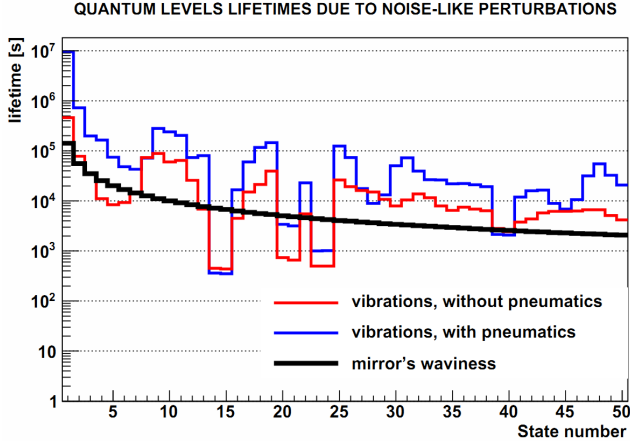


Fig. 11. (color online) The partial lifetime of neutrons in a gravitational quantum state as a function of the state number in standard conditions with/without anti-vibration pneumatics are shown with blue and red lines. Black line indicates the estimated partial lifetimes defined by the mirror waviness.

### 2.8. Transitions between quantum states caused by vibration noise

Two effects — vibrations and waviness of the mirrors — could decrease storage times of UCNs in gravitational quantum states. They are described by common formalism.<sup>45</sup> While the mirror waviness could be only estimated theoretically at the moment as the mirrors are still in production, spectra of vibrations have been measured in realistic conditions of the GRANIT spectrometer already installed to its permanent position in the ILL reactor hall. Figure 11 shows the lifetime of neutrons in 50 lowest quantum states in standard conditions. Natural mechanical and human-made vibration noise were found to present no concern for stability of the quantum states. Only deliberate shocks against the apparatus would drastically spoil the experiment.

## 3. New Methodical Developments for GRANIT

New methodical developments for the GRANIT spectrometer<sup>29,2</sup> address eventual further improvements of some critical parameters of this experimental installation, as well as its applications to new fields of research. Keeping in mind an extremely small fraction of UCN that could be bound in gravitational quantum states, we look for methods to increase statistics due to developing UCN sources with maximum phase-space density<sup>30–32</sup> and counting simultaneously a large fraction of neutrons using position-sensitive detectors.<sup>15,46,4</sup> On the other hand, we have to reduce backgrounds in our UCN detectors.<sup>36,4</sup> Significant efforts are devoted to develop neutron optics<sup>37,36</sup> for GRANIT, and spectrum-shaping devices.<sup>41–44</sup> Also we explore an eventual application of the GRANIT spectrometer beyond the scope of its initial goals, such as, for instance, constraining short-range interactions<sup>47,48,5</sup>

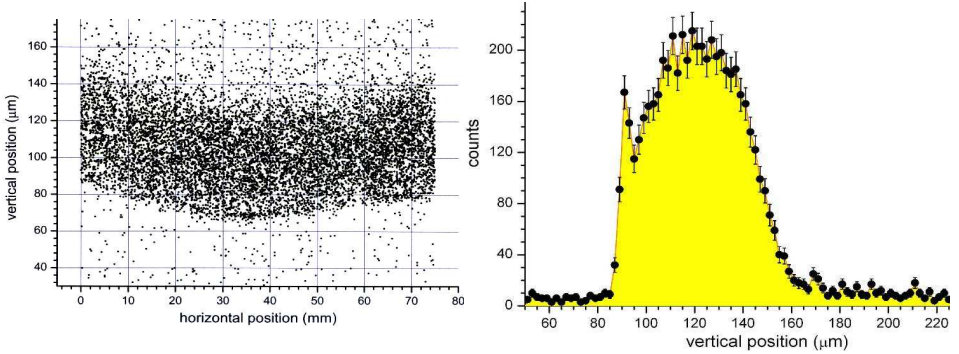


Fig. 12. Track distribution in a CR39 detector with a  $^{235}\text{U}$  converter. Left panel — raw track coordinate distribution; right panel — vertical track distribution after applying a correction for the detector shape deformation.

using gravitational and centrifugal<sup>26–28,7</sup> quantum states of neutrons: it might be used, for instance, for prototyping experiments with gravitational quantum states of anti-hydrogen,<sup>33</sup> or as a UCN general-purpose reflectometer.

The principle method for observing gravitational quantum states of neutrons in the first experiments<sup>16–18</sup> consisted of studying wave functions of neutrons in quantum states.

### 3.1. Nuclear-track position-sensitive detectors

Currently, detectors of only one type provide the highest spatial resolution of  $\sim 1 \mu\text{m}$ , reasonably high efficiency of at least several tens percent, long sensitive zone of several tens centimeters, and extremely low background, needed for direct measurements of these wave functions: nuclear-track detectors with thin converters, for instance, of  $^{235}\text{U}$ ,  $^{10}\text{B}$ ,  $^7\text{Li}$  (using the nuclear reactions:  $^6\text{Li}(n, ^3\text{H})^4\text{He}$ ,  $^{10}\text{B}(n, ^4\text{He})^7\text{Li}$ ,  $^{235}\text{U}(n, \text{fission})$  with following detection of tracks produced by charged particles).<sup>15,4</sup> Careful analysis of operation of such detectors as well as comparison of various options could be found in Ref. 4. An example taken from Ref. 4 in Fig. 12 proves the feasibility of using such nuclear-track detectors for reconstruction of wave functions of neutrons in gravitational quantum states.

### 3.2. Analysis of measured neutron probability distributions

The data shown in Fig. 12 could be analyzed in terms of extracting parameters of the neutron wave functions contributing to the result. The characteristic spatial extensions of wave functions in lowest quantum states is  $z_0 = \sqrt[3]{\hbar^2/2m^2g} = 5.87 \mu\text{m}$ ; the wave functions could be represented in terms of  $z_0$ . As lowest quantum states, except for the first state, exhibit nodes at the height of  $\sim 10 \mu\text{m}$ , they contribute coherently to the node at  $\sim 10 \mu\text{m}$ . Removal of the lowest quantum state allows one to use statistics of several quantum states to measure the height of the node.<sup>49</sup>

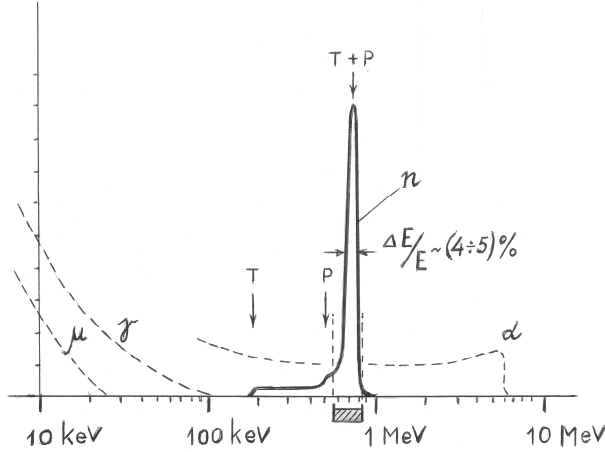


Fig. 13. A typical differential amplitude spectrum of the electrical signals at the electrodes in a UCN gaseous detector filled in with gaseous mixture containing  $^3\text{He}$ ; the detector is operated in the proportional counter regime. The amplitude of the electrical signal is shown on the  $y$ -axis, the ionization energy is given on the  $x$ -axis. The energies of triton ( $T$ ), proton ( $p$ ), and the total reaction energy ( $T + p$ ) are indicated with arrows. Spectra of background  $\alpha$ -particles,  $\gamma$ -quanta, and muons are shown with dashed lines.

Moreover, partial population of every quantum state could be fitted from the spectrum shape, and thus corrections could be introduced taking into account shifts in the node height for every state. The statistical accuracy of extracting  $z_0$  in such a way is quite high:  $z_0 = 5.9 \pm 0.2 \mu\text{m}$ . Measurements of this kind with equal, or lower, systematic uncertainties are previewed with the GRANIT spectrometer.

### 3.3. Low-background counters of UCN

The first method for studying neutron wave functions in Refs. 16–18 consisted of measuring flux of UCN through the slit between a horizontal mirror on bottom and a rough absorber/scatterer on top, as a function of the slit height. A typical result of such an experiment is shown in Fig. 10 (copied from Ref. 18). In spite of using the most intense UCN source (PF2 instrument at ILL) and also optimizing the neutron transport losses, the count rate in the data shown in Fig. 10 is very low. This measurement was feasible only due to using neutron counters with even lower backgrounds described in Ref. 4. A typical “resonance-like” amplitude spectrum in such a detector is given in Fig. 13 and the detector is sketched in Fig. 14.

### 3.4. Real-time position-sensitive UCN detectors

Provided an equivalent spatial resolution is achieved, real-time position-sensitive detectors would have evident advantages over nuclear-track detectors. That is why serious efforts are devoted to improve their spatial resolution to the level of  $\sim 1 \mu\text{m}$ , characteristic for nuclear-track detectors today.<sup>4</sup> The best real-time spatial

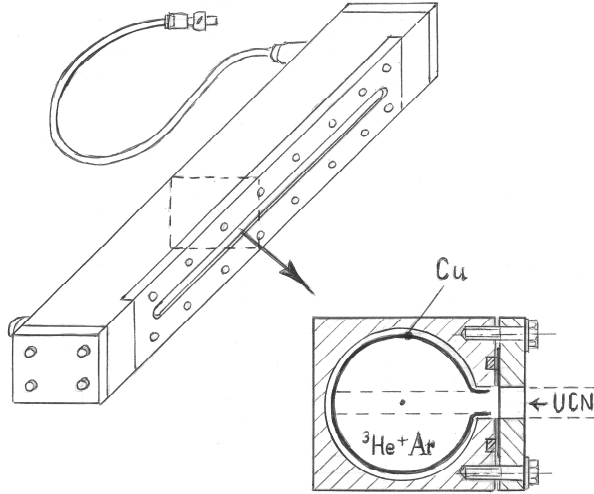


Fig. 14. A scheme of the GRANIT low-background neutron gaseous proportional counter.

resolution of  $5.3 \mu\text{m}$  achieved so far and high, close to unity, efficiency of UCN detection are reported for solid-state detectors with  $^{10}\text{B}$  and  $^6\text{Li}$  convertors.<sup>46,21</sup> One such detector is Timepix; it is a planar pixilated semiconductor detector, with the thickness of 0.3–1 mm, bump-bonded to a Medipix readout chip. The pixel size in a Timepix detector is 55 by 55  $\mu\text{m}^2$ ; the maximum surface area is 3 by 3  $\text{cm}^2$ . The charged particle track coordinates are read out using the Subpixel resolution technology.

### 3.5. UCN reflectometry, elastic and inelastic neutron scattering, AC magnetometry

Neutron reflectometry is a well-recognized tool commonly used to study structural organization of various thin films and multilayers (see, for instance, a review by Zabel *et al.*<sup>50</sup>). Neutrons penetrate deeply into films and, being specularly reflected from layer's interface, record the scattering length density profile across the depth of the film, or multilayer. A lateral configuration of layers is additionally accessible via resolving scattering in off-specular directions. The range of off-specular scattering is dramatically enhanced for longer wavelengths. For UCN it covers the total solid angle. We study feasibility of using UCN reflectometry to address interesting problems in nanoscience, e.g. those related to magnetic dynamics and kinetics in nano-patterns.<sup>4</sup> In particular, AC magnetometry with polarized neutron scattering is a tool applied to probe frequency dispersive properties of various materials, e.g. nanostructures employed in spintronic devices; the method is based on measurements of magnetization response to the external magnetic field changing with time.

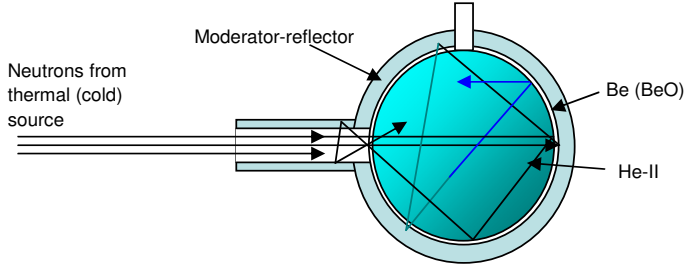


Fig. 15. A principal scheme of “external” cold neutron source for UCN super-thermal helium source.

Special *UCN beam shaping* is needed in order to use the GRANIT spectrometer in the mode of UCN reflectometer; also it might be useful in order to deliver highest phase-space density to experiments with gravitational quantum states of neutrons. While a method of semi-diffusive slit<sup>31,32</sup> (a mirror on bottom and a scatterer/reflector on top) was proposed and tested for efficiently extracting UCN from the UCN source to the GRANIT spectrometer, it provides a “white” spectrum of horizontal velocity components. Thus this method could not be directly used for spectral reflectometry measurements.<sup>4</sup>

### 3.6. “Virtual” cold neutron source

In order to increase UCN density delivered to the GRANIT spectrometer we develop several options. One option is based on the idea of external “virtual” cold neutron source illustrated in Fig. 15 and consisting of the following. Instead of putting a super-thermal helium UCN source<sup>51</sup> in an external neutron beam (with its relatively low neutron flux), or inside the thermal neutron source (with its high heating and safety problems), we could put it inside a reflecting cryogenic cavity at the exit of a thermal neutron guide.<sup>4</sup> Such a configuration allows: considerable increase in the total flux of 8.9 Å neutrons in the cavity due to neutron albedo also due to neutron cooling in the reflector/moderator material, large increase in UCN storage times and decrease in transport losses of thermal and UCNs.

The new method of *nanoparticle reflectors*<sup>52–56</sup> allows decreasing transport losses of very cold and cold neutrons; and could be used for neutron reflectors. Figure 16 is copied from Ref. 54; it illustrates albedo of neutrons from nano-diamond reflectors and compares it to properties of other known reflectors.

## 4. Short-Range Fundamental Forces

We reproduce here two figures summarizing present status of experimental constraints for spin-independent (Fig. 17) and spin-dependent (Fig. 18) short-range interactions (updated by new results from Ref. 60 shown as line 3 in Fig. 17) and refer readers for a detailed description to GRANIT-2010 proceedings.<sup>5</sup>

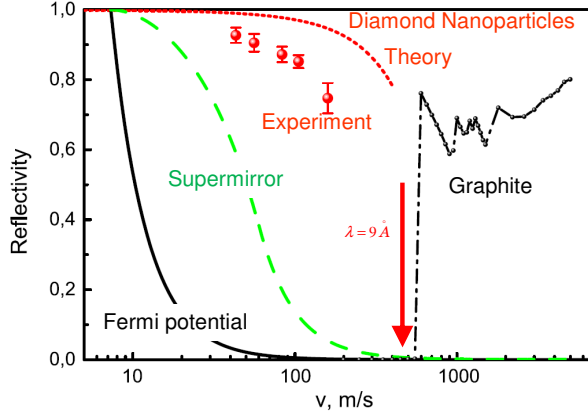


Fig. 16. The elastic reflection probability for isotropic neutron flux is shown as a function of the neutron velocity for various carbon-based reflectors: (i) DLC (thin solid line), (ii) the best supermirror<sup>57</sup> (dashed line), (iii) hydrogen-free ultradiamond powder with the infinite thickness (dotted line). Calculation. (iv) VCN reflection from 3 cm thick diamond nano-powder at the ambient temperature (points), with significant hydrogen contamination Experiment.<sup>54</sup> (v) MCNP calculation for reactor graphite reflector<sup>58</sup> with the infinite thickness at the ambient temperature.

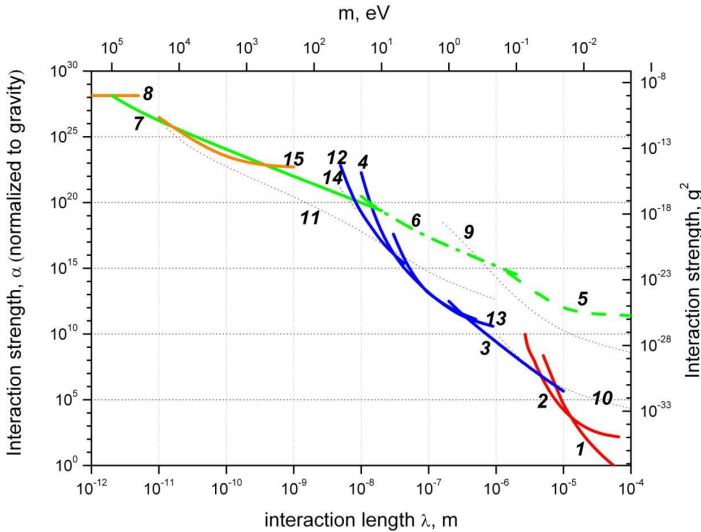


Fig. 17. (color online) The exclusion plot for new spin-independent interactions: the interaction strength  $\alpha$ , normalized to the gravitational interaction (on left), and the interaction strength  $g^2$  (on right) is given as a function of the characteristic distance. The best currently available constraints are shown in thick solid lines; preliminary results are indicated in thick dash-dotted lines; the best neutron constraints, but not the best currently available, are given in thick dashed lines; thin dotted lines in purple color correspond to projected sensitivity in various neutron experiments. Red color is reserved for measurements of gravity at short distances; blue-color constrains result from precision measurements of Casimir interactions; all constraints originated from neutron experiments are shown in green; constraint from measurements of exotic atoms, and those with neutrino detectors, is indicated in orange. Each constraint (1–15) is commented in detail in Ref. 5.

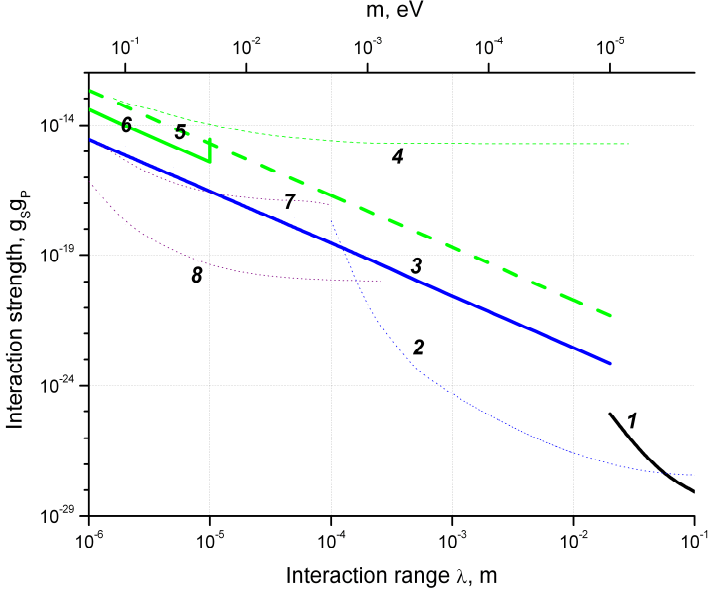


Fig. 18. (color online) Searches for short-range nucleon spin-dependent interactions. The style of lines is analogous to that used in Fig. 17. Limits 1, 2, 3 are derived from atomic experiments. Limits 4, 5, 6 are obtained using experiments with neutrons. Limits 7 and 8 could be obtained using the GRANIT spectrometer, at first stage and the ultimate sensitivity accordingly. Each constraint (1–8) is commented in detail in Ref. 5.

A particularly interesting kind of extra fundamental force, that could be verified using results of the GRANIT experiment, is “chameleons”, as analyzed in Ref. 59. Chameleons are called so due to the screening of this extra force at distances larger than some characteristic value.

## 5. Conclusion

We overviewed here recent developments concerning gravitational quantum states of neutrons and the GRANIT spectrometer. These topics were discussed in detail during recent GRANIT-2010 Workshop in Les Houches; readers could get more information in the proceedings and materials of this Workshop.

## Acknowledgment

The GRANIT spectrometer is constructed in framework of an ANR (Agence Nationale de la Recherche, France) grant BLANC ANR-05-BLAN-0098-01 received in 2005 by a collaboration ILL-LPSC-LMA.<sup>29</sup> Permanent installation of the GRANIT spectrometer at the ILL high-flux reactor is financed by ILL and IN2P3 institutes. Important contributions came from University of Virginia (e.g. through NSF grant PHY-0855610), PNPI, JINR and other collaborators.



The author is grateful to ILL/IN2P3/ANR for support of this activity, and all members of the GRANIT collaboration and participants of the GRANIT-2010 Workshop for contributions to this research.

## References

1. I. Antoniadis *et al.*, *C. R. Phys.* **12**, 703 (2011).
2. S. Baessler *et al.*, *C. R. Phys.* **12**, 707 (2011).
3. <http://www.ill.eu>.
4. S. Baessler *et al.*, *C. R. Phys.* **12**, 729 (2011).
5. I. Antoniadis *et al.*, *C. R. Phys.* **12**, 755 (2011).
6. Th. Bourdel *et al.*, *C. R. Phys.* **12**, 779 (2011).
7. V. V. Nesvizhevsky and A. Yu. Voronin, *C. R. Phys.* **12**, 791 (2011).
8. <http://lpsc.in2p3.fr/Indico/conferenceDisplay.py?ovw=True&confId=371>.
9. V. I. Luschikov *et al.*, *JETP Lett.* **9**, 23 (1969).
10. V. K. Ignatovich, *The Physics of Ultracold Neutrons* (Clarendon Press, 1990).
11. R. Golub, D. J. Richardson and S. K. Lamoreaux, *Ultracold Neutrons* (Adam Higler, 1991).
12. I. I. Goldman *et al.*, *Problems in Quantum Mechanics* (Academic Press, 1960).
13. V. I. Luschikov and A. I. Frank, *JETP Lett.* **28**, 559 (1978).
14. J. J. Sakurai, *Modern Quantum Mechanics* (Benjamin/Cummings, 1985).
15. V. V. Nesvizhevsky *et al.*, *Nucl. Instrum. Meth. A* **440**, 754 (2000).
16. V. V. Nesvizhevsky *et al.*, *Nature* **415**, 297 (2002).
17. V. V. Nesvizhevsky *et al.*, *Phys. Rev. D* **67**, 102002 (2003).
18. V. V. Nesvizhevsky *et al.*, *Eur. Phys. J. C* **40**, 479 (2005).
19. S. Baessler, *J. Phys. G: Nucl. Part. Phys.* **36**, 104005 (2009).
20. V. V. Nesvizhevsky *et al.*, *Phys. Usp.* **53**, 645 (2010).
21. T. Sanuki *et al.*, *Nucl. Instrum. Meth. A* **600**, 657 (2009).
22. T. Jenke *et al.*, *Nucl. Instrum. Meth. A* **611**, 318 (2009).
23. M. Kreuz *et al.*, *Nucl. Instrum. Meth. A* **611**, 326 (2009).
24. V. V. Nesvizhevsky and K. V. Protasov, Quantum states of neutrons in the earth's gravitational field: State of the art, applications, perspectives, in *Trends in Quantum Gravity Research* (Nova Science Publishers, 2006).
25. T. Jenke *et al.*, *Nat. Phys.* **7**, 468 (2011).
26. V. V. Nesvizhevsky *et al.*, *Phys. Rev. A* **78**, 033616 (2008).
27. V. V. Nesvizhevsky *et al.*, *Nat. Phys.* **6**, 114 (2010).
28. V. V. Nesvizhevsky *et al.*, *New J. Phys.* **12**, 113050 (2010).
29. V. V. Nesvizhevsky, K. V. Protasov and J. M. Mackowski, Project BLANC ANR-05-BLAN-0098-01 (2005-2009).
30. P. Schmidt-Wellenburg *et al.*, *Nucl. Instrum. Meth. A* **611**, 267 (2009).
31. J. Barnard *et al.*, *Nucl. Instrum. Meth. A* **591**, 431 (2008).
32. P. Schmidt-Wellenburg *et al.*, *Nucl. Instrum. Meth. A* **577**, 623 (2007).
33. A. Yu. Voronin, *Phys. Rev. A* **83**, 032903 (2011).
34. P. Courtois *et al.*, *Nucl. Instrum. Meth. A* **634**, 537 (2011).
35. G. Pignol, Ph.D. thesis, Joseph Fourier University, Grenoble (2009).
36. V. V. Nesvizhevsky *et al.*, *Nucl. Instrum. Meth. A* **557**, 576 (2006).
37. V. V. Nesvizhevsky *et al.*, *Nucl. Instrum. Meth. A* **578**, 435 (2007).
38. Grenoble: ILL experimental report TEST-691 (2004).
39. D. G. Kartashov *et al.*, *Int. J. Nanosci.* **6**, 501 (2007).
40. V. V. Nesvizhevsky *et al.*, preprint (2007), arXiv:0708.2541.

41. A. Yu. Voronin *et al.*, *Phys. Rev. D* **73**, 044029 (2006).
42. A. E. Meyerovich *et al.*, *Phys. Rev. A* **73**, 063616 (2006).
43. R. Adhikari *et al.*, *Phys. Rev. A* **75**, 063613 (2007).
44. M. Escobar and A. E. Meyerovich, *Phys. Rev. A* **83**, 033618 (2011).
45. C. Codau *et al.*, accepted for publication in *Nucl. Instrum. Meth. A*.
46. J. Jakubek *et al.*, *Nucl. Instrum. Meth. A* **600**, 651 (2009).
47. S. Baessler *et al.*, *Phys. Rev. D* **75**, 075006 (2007).
48. V. V. Nesvizhevsky *et al.*, *Phys. Rev. D* **77**, 034020 (2008).
49. V. V. Nesvizhevsky, *Phys. Usp.* **47**, 515 (2004).
50. H. Zabel, K. Theis-Brohl and B. P. Toperverg, *Handbook of Magnetism and Advanced Magnetic Materials*, Vol. 1, eds. H. Kronmuller and S. Parkin (John Wiley and Sons, 2007).
51. R. Golub *et al.*, *Phys. Lett. A* **62**, 337 (1977).
52. V. V. Nesvizhevsky, *Phys. Atom. Nucl.* **65**, 400 (2002).
53. V. V. Nesvizhevsky *et al.*, *Nucl. Instrum. Meth. A* **595**, 631 (2008).
54. E. V. Lychagin *et al.*, *Phys. Lett. B* **679**, 186 (2009).
55. R. Cubitt *et al.*, *Nucl. Instrum. Meth. A* **622**, 182 (2010).
56. A. R. Krylov *et al.*, *Crystallogr. Rep.* **56**, 102 (2011).
57. R. Maruyama *et al.*, *Thin Solid Films* **515**, 5704 (2007).
58. E. Fermi, *A Course in Neutron Physics* (The University of Chicago Press, 1965).
59. P. Brax and G. Pignol, *Phys. Rev. Lett.* **107**, 111301 (2011).
60. A. O. Sushkov *et al.*, *Phys. Rev. Lett.* **107**, 171101 (2011).